High Pressure Research
Vol. 32, No. 2, June 2012, 262–269

Taylor & Francis
Taylor & Francis Group

High pressure X-ray diffraction study on $BaWO_4$-II

Dayong Tan[a], Wansheng Xiao[a]*, Wei Zhou[a], Ming Chen[a], Wenge Zhou[b], Xiaodong Li[c], Yanchun Li[c] and Jing Liu[c]

[a]*Guangzhou Institute of Geochemistry, Chinese Academy of Sciences, Guangzhou 510640, China;* [b]*Institute of Geochemistry, Chinese Academy of Sciences, Guiyang 550002, China;* [c]*Institute of High Energy Physics, Chinese Academy of Sciences, Beijing 100049, China*

(*Received 19 October 2011; final version received 16 January 2012*)

$BaWO_4$-II has been synthesized at 5 GPa and 610°C. Its high pressure behavior was studied by *in situ* synchrotron X-ray diffraction measurements at room temperature up to 17 GPa. $BaWO_4$-II retains its monoclinic structure. Bulk and axial moduli determined by fitting a third-order Birch–Murnaghan equation of state to lattice parameters are: $K_0 = 86.2 \pm 1.9$ GPa, $K_0(a) = 56.0 \pm 0.9$ GPa, $K_0(b) = 85.3 \pm 2.4$ GPa, and $K_0(c) = 146.1 \pm 3.2$ GPa with a fixed $K' = 4$. Analysis of axial compressible modulus shows that the *a*-axis is 2.61 times more compressible than the *c*-axis and 1.71 times more compressible than the *b*-axis. The beta angle decreases smoothly between room pressure and 17 GPa from 93.78° to 90.90°.

Keywords: $BaWO_4$-II; equation of state; synchrotron X-ray diffraction; high pressure

1. Introduction

Scheelite-type structure (space group [SG]: $I4_1/a$, No. 88, $Z = 4$) plays a significant role in mineralogy, materials science, and geoscience. Under ambient conditions, a large number of ABO_4-type tungstates and molybdates crystallize in this structure [1]. Many other ABO_4 compounds with zircon ($I4_1/amd$), monazite ($P2_1/n$), and $CrVO_4$-type structures ($Cmcm$) transform to the scheelite polymorph at high pressure [2]. The pressure effects on the structural and electronic properties of scheelite-type ABO_4 crystals have attracted wide interest of researchers, and a pressure-induced structural sequence scheelite → fergusonite → $P2_1/n$ → $BaMnF_4$ → $Cmca$ has been explored [3]. $BaWO_4$-II (SG: $P2_1/n$, No. 14, $Z = 8$) as a high pressure polymorphism of scheelite-structured barium tungstate has been synthesized as early as the 1970s at pressures of 4.3–5.5 GPa and temperatures of 600–1000°C [4,5]. Later, the monoclinic $BaWO_4$-II has also been obtained at about 10 GPa and room temperature [6,7]. However, we found an inconsistency in the stability of $BaWO_4$-II based on reversibility and irreversibility of the reported $BaWO_4$-II. $BaWO_4$-II was obtained at room temperature and high pressure (RT-HP), reverting to the initial

*Corresponding author. Email: wsxiao@gig.ac.cn

ISSN 0895-7959 print/ISSN 1477-2299 online

http://dx.doi.org/10.1080/08957959.2012.658789
http://www.tandfonline.com

scheelite phase while unloading pressure [6,7]; whereas, it was synthesized at high temperature and high pressure (HT-HP) can be quenched to ambient conditions [4,5].

In order to clarify the stability of the $BaWO_4$-II phase, we carried out the Raman measurements of $BaWO_4$-II at room temperature up to 14.8 GPa [8]. The experimental results show that $BaWO_4$-II retains its monoclinic structure. Lacomba-Perales *et al*. [9] carried out the experimental and theoretical investigation of the stability of the monoclinic $BaWO_4$-II under high pressure and high temperature. The authors confirmed that $BaWO_4$-II phase is the stable HT-HP structure of $BaWO_4$. So far, the structural stability of $BaWO_4$-II at room temperature has not been examined by other techniques and its compressibility has not been measured. In this study, we have prepared $BaWO_4$-II and carried out the angle-dispersive X-ray diffraction (ADXRD) measurements up to 17 GPa to explore its structural stability and compressibility as well as expect that the high pressure diffraction data of $BaWO_4$-II will provide help for identifying the post-fergusonite structure of $BaWO_4$ at the RT-HP experiments.

2. Experimental

The sample of $BaWO_4$-II was synthesized at 5 GPa and 610°C for 8 h with a cubic-anvil apparatus. Scheelite-structured $BaWO_4$ was used as a starting material and sealed in a copper capsule. The X-ray diffraction and Raman measurements of the quenched product indicate that it is a pure $BaWO_4$-II phase [8].

The ADXRD patterns were collected at the 4W2 High pressure station of the Beijing Synchrotron Radiation Facility (BSRF), and BL-18C station at the Photon Factory, High Energy Accelerator Research Organization (KEK) with monochromatic X-ray beam $\lambda = 0.6199$ and 0.6198 Å, respectively. A symmetric Mao-Bell-type diamond anvil cell (DAC) with 400 μm culet diamond anvils was used in the high pressure experiments. The T301 stainless steel gasket was pre-indented to an initial thickness of about 50 μm and then drilled to give a 120 μm hole serving as the sample chamber. The synthesized $BaWO_4$-II was ground to fine powder, and the powder was pressed into small pellets by the diamond anvils prior to the setting of the gasket. The small $BaWO_4$-II pellet and a ruby chip were loaded into the sample chamber. A methanol–ethanol–water (16:3:1) mixture was used as a pressure-transmitting medium. The pressure was measured by the shift of the R1 photoluminescence line of ruby [10]. Rietveld refinements of the diffraction data at 9.6 and 15.6 GPa were performed using the GSAS package [11].

3. Results and discussion

The ADXRD spectra of $BaWO_4$-II at a few representative pressures are shown in Figure 1. With increasing pressure, all the Bragg diffraction lines shift continuously toward higher 2θ angles and no additional diffraction peaks appear. Careful observation of the selected range of 2θ angles in Figure 1 reveals that there was some splitting or merging of the diffraction peaks. The change in intensity of the diffraction peaks might be due to the differences in the atomic moving manner. The Rietveld refinement of the $BaWO_4$-II phase at pressures of 9.6 and 15.6 GPa were carried out with residual parameters $\chi^2 = 0.1044$, $R_p = 4.23\%$, $R_{wp} = 5.72\%$, and $\chi^2 = 0.1219$, $R_p = 3.59\%$, $R_{wp} = 4.96\%$, respectively. The diffraction patterns are shown in Figure 2. Comparing the detailed structural parameters of $BaWO_4$-II phase at high pressure in Table 1 with that at ambient pressure in Ref. [4], we found that the WO_6 octahedra are slightly distorted and the average W_1-O and W_2-O bond length changes slightly from 1.97 and 1.98 Å at ambient pressure to 1.9409 and 1.9529 Å at 9.6 GPa and to 1.9345 and 1.9473 Å at 15.6 GPa, respectively. On the contrary, the BaO_{8-9} polyhedrons have a large compression, the average Ba_1-O and Ba_2-O bond length reduces from

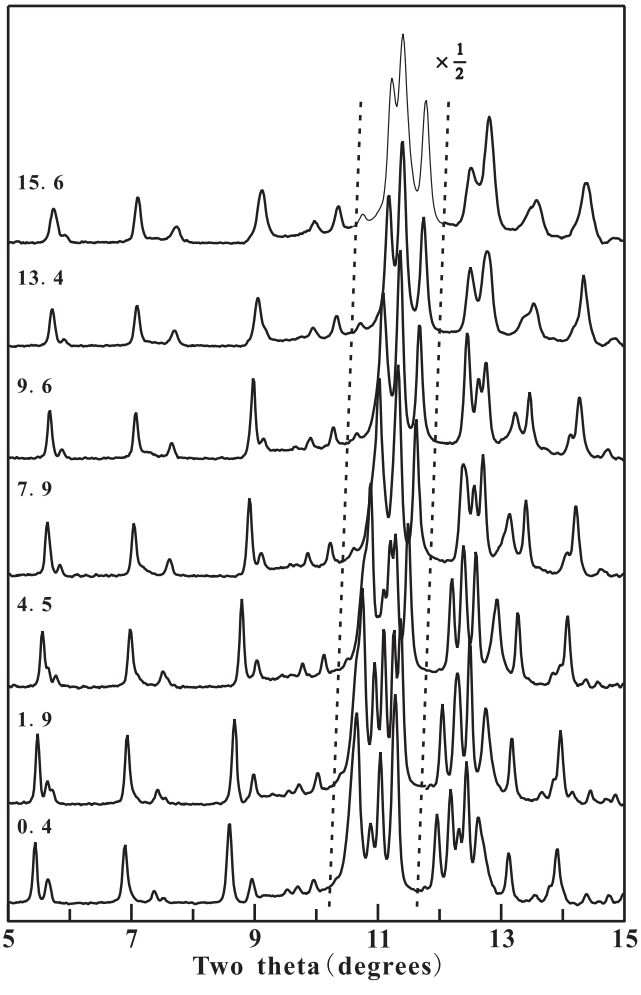

Figure 1. Representative X-diffraction spectra of $BaWO_4$-II at a few pressures. The numbers above patterns are corresponding pressures in GPa.

2.83 and 2.76 Å at ambient pressure to 2.7126 and 2.6287 Å at 9.6 GPa and to 2.6786 and 2.5891 Å at 15.6 GPa, respectively. The change in internal parameters induces change in the intensity of diffraction peaks, but all the X-ray diffraction patterns have a close similarity with increasing pressure. So, the observed facts suggest that no phase transition takes place in $BaWO_4$-II with pressures up to 17 GPa at room temperature. This result is well consistent with the high pressure Raman studies of $BaWO_4$-II [8].

In order to obtain the lattice parameters of $BaWO_4$-II, we index observable 24 reflection lines at low angles (5–14°). From the analysis of X-ray diffraction data, we extracted the lattice parameters of $BaWO_4$-II at different pressures (listed in Table 2). In Figures 3 and 4, the lattice parameters (except the beta angle) normalized by ambient pressure values are plotted as a function of pressure. The smooth curves of cell lattices and beta angle in Figure 3 reveal that there is no phase transition in the pressure range of our experiments, and the compression behavior of the $BaWO_4$-II phase is highly anisotropic. The axis compressible modulus parameters ($K_0(a) = 56.0 \pm 0.9$ GPa, $K_0(b) = 85.3 \pm 2.4$ GPa, and $K_0(c) = 146.1 \pm 3.2$ GPa), which were obtained by fitting a "linearized" third-order Birch–Murnaghan EoS [12], show that a-axis is about 2.61 times larger than that of

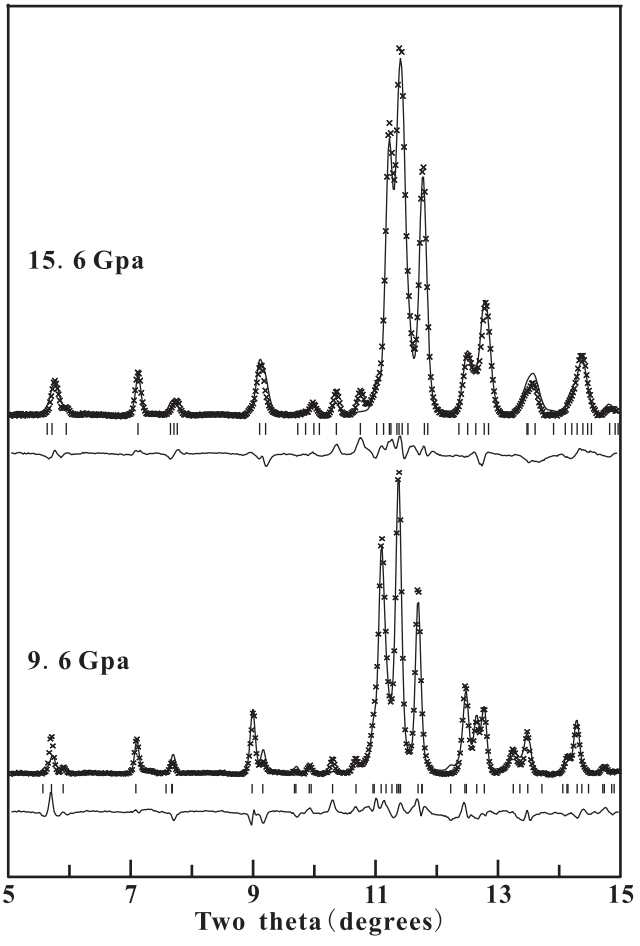

Figure 2. Observed, calculated, and difference X-ray diffraction patterns for the $BaWO_4$-II phase at 9.6 and 15.6 GPa. Bars indicate the expected positions of diffraction peaks.

the c-axis and 1.71 times larger than that of the b-axis. For the monoclinic $BaWO_4$-II (SG $P2_1/n$, No. 14, $Z = 8$), it is built up of zigzag layers of WO_6 octahedra parallel to the a-axis; the zigzag layer consists of eight- and four-membered rings of WO_6 octahedra by edge- and corner-sharing; adjacent layers are linked by barium atoms. The fact that the a-axis is much more compressible than the other axes indicates that there is a significant shortening of the Ba−O bond. Figure 3 also shows that the beta angle from initial 93.78° decreases to 90.90° with increasing pressure.

A least-squares fit of unit-cell volume as a function of pressure to a third-order Birch–Murnaghan equation of state [13] is given as

$$P = \frac{3}{2}K_0\left[\left(\frac{V_0}{V}\right)^{7/3} - \left(\frac{V_0}{V}\right)^{5/3}\right]\left\{1 + \frac{3}{4}(K' - 4)\left[\left(\frac{V_0}{V}\right)^{2/3} - 1\right]\right\},$$

where P, V_0,K_0, and K' are the pressure, zero-pressure volume, isothermal bulk modulus, and the pressure derivative of isothermal bulk modulus, respectively. Our results with the data collected below 17 GPa suggests that $K_0 = 86.2 \pm 1.9$ GPa with a fixed unit cell volume $V_0 = 704.72$ Å^3 and pressure derivatives $K' = 4$. Since the data gathered at pressures above 10 GPa were potentially affected by the non-hydrostatic stress in the diamond cell as the solidification of the pressure

Table 1. Lattice parameters for $BaWO_4$-II phase at 9.6 and 15.6 GPa.

Atom	Site	x	y	z	Atom	Site	x	y	z
Structural parameters of $BaWO_4$-II at 9.6 GPa: $P2_1/n$, $Z = 8$, $a = 12.547(4)$ Å, $b = 6.910(1)$ Å, $c = 7.342(2)$ Å, $\beta = 91.62(2)^\circ$									
Ba_1	4e	0.1647	0.6599	0.1633	Ba_2	4e	0.1499	0.9434	0.6487
W_1	4e	0.0874	0.1645	0.0989	W_2	4e	0.0921	0.4521	0.6619
O_1	4e	0.1160	0.0314	0.3041	O_2	4e	0.1814	0.5920	0.8042
O_3	4e	0.0593	0.6426	0.4774	O_4	4e	0.2179	0.2599	0.0640
O_5	4e	0.0568	0.2778	0.8304	O_6	4e	0.1785	0.3164	0.5291
O_7	4e	0.0288	0.3720	0.1956	O_8	4e	0.0809	0.9373	0.9560
Bond lengths (Å)									
W_1-O_1	1.7921(3)	W_2-O_2	1.7936(3)	Ba_1-O_1	2.8406(3)	Ba_2-O_1	2.6250(6)		
W_1-O_4	1.7901(5)	W_2-O_3	1.9252(3)	Ba_1-O_2	2.6920(6)	Ba_2-O_2	2.7073(3)		
W_1-O_5	2.1461(5)	W_2-O_3	2.2296(6)	Ba_1-O_3	2.6929(6)	Ba_2-O_2	2.3688(7)		
W_1-O_7	1.7694(2)	W_2-O_5	1.7906(3)	Ba_1-O_4	2.9399(3)	Ba_2-O_3	2.6672(3)		
W_1-O_8	1.8986(2)	W_2-O_6	1.7510(3)	Ba_1-O_4	2.5474(6)	Ba_2-O_4	2.6347(5)		
W_1-O_8	2.2491(7)	W_2-O_7	2.2273(4)	Ba_1-O_5	2.8140(9)	Ba_2-O_5	2.9281(4)		
				Ba_1-O_6	2.6822(6)	Ba_2-O_6	2.7497(3)		
				Ba_1-O_7	2.6349(4)	Ba_2-O_8	2.4234(6)		
				Ba_1-O_8	2.6572(4)				
Average	1.9409	Average	1.9529	Average	2.7126	Average	2.6287		
Structural parameters of $BaWO_4$-II at 15.6 GPa: $P2_1/n$, $Z = 8$, $a = 12.327(4)$ Å, $b = 6.861(1)$ Å, $c = 7.307(1)$ Å, $\beta = 90.92(1)^\circ$									
Ba_1	4e	0.1671	0.6622	0.1657	Ba_2	4e	0.1523	0.9458	0.6511
W_1	4e	0.0898	0.1669	0.1014	W_2	4e	0.0944	0.4545	0.6643
O_1	4e	0.1184	0.0338	0.3065	O_2	4e	0.1838	0.5944	0.8066
O_3	4e	0.0617	0.6450	0.4798	O_4	4e	0.2203	0.2623	0.0664
O_5	4e	0.0592	0.2802	0.8328	O_6	4e	0.1809	0.3188	0.5315
O_7	4e	0.0312	0.3744	0.1980	O_8	4e	0.0833	0.9397	0.9560
Bond lengths (Å)									
W_1-O_1	1.7854(2)	W_2-O_2	1.7830(3)	Ba_1-O_1	2.8171(3)	Ba_2-O_1	2.6165(4)		
W_1-O_4	1.7590(5)	W_2-O_3	1.9164(2)	Ba_1-O_2	2.6765(5)	Ba_2-O_2	2.6906(3)		
W_1-O_5	2.1389(3)	W_2-O_3	2.2836(5)	Ba_1-O_3	2.6579(5)	Ba_2-O_2	2.2795(6)		
W_1-O_7	1.7507(2)	W_2-O_5	1.7751(2)	Ba_1-O_4	2.9157(3)	Ba_2-O_3	2.6511(3)		
W_1-O_8	1.8870(2)	W_2-O_6	1.7255(3)	Ba_1-O_4	2.4786(4)	Ba_2-O_4	2.5797(4)		
W_1-O_8	2.2883(6)	W_2-O_7	2.1999(4)	Ba_1-O_5	2.8175(8)	Ba_2-O_5	2.8970(3)		
				Ba_1-O_6	2.6132(5)	Ba_2-O_6	2.7289(3)		
				Ba_1-O_7	2.6028(4)	Ba_2-O_8	2.3982(4)		
				Ba_1-O_8	2.6436(4)				
Average	1.9349	Average	1.9473	Average	2.6786	Average	2.5891		

media at about 10 GPa [14]. The data gathered at pressure below 10 GPa fitted to the third-order Birch–Murnaghan equation of state yielding a volume of $V_0 = 703.0 \pm 0.6$ Å^3, an isothermal bulk modulus of $K_0 = 67.7 \pm 2.6$ GPa, and first pressure derivative of $K' = 7.3 \pm 0.8$. If K' is fixed at 4, then K_0 is obtained as 76.7 ± 0.7 GPa.

Panchal *et al*. [15] and Errandonea *et al*. [6] observed that scheelite-structured $BaWO_4$ transforms to fergusonite at about 7.1 GPa. Further increasing pressure above 10 GPa, they also found evidence that $BaWO_4$ occurs another phase transition. Errandonea *et al*. [6] have proposed, based on the LeBail refinement of the ADXRD pattern of $BaWO_4$, that the new high pressure phase is the $BaWO_4$-II structure; the lattice parameters at 10.9 GPa are: $a = 12.841(9)$ Å, $b = 7.076(6)$ Å, $c = 7.407(6)$ Å, and $\beta = 93.0(9)^\circ$. In a recent study, Lacomba-Perales *et al*. [9] presented the cell volume of $BaWO_4$-II at 6 GPa and different temperatures.

Figure 4 shows the collected data of $BaWO_4$-II in this work and previous studies. The solid and empty circles correspond to the data obtained at BL-18C and 4W2, respectively. Two sets of data were fitted by a quadratic polynomial. The coefficient of determination ($R^2 = 0.9971$) suggests that the experimental data has a good linear correlation. The solid triangle corresponds

Table 2. Lattice parameters collected at different pressures for $BaWO_4$-II.

P (GPa)	*a* (Å)	*b* (Å)	*c* (Å)	Beta (°)	*V* (Å^3)
0.0001[a]	13.154(2)	7.162(1)	7.497(1)	93.78(1)	704.7(1)
0.38[b]	13.100(4)	7.140(2)	7.482(3)	93.63(3)	698.3(3)
1.05[a]	13.054(3)	7.117(2)	7.465(2)	93.16(3)	692.5(2)
1.08[b]	13.055(4)	7.116(2)	7.465(3)	93.40(4)	692.3(3)
1.92[b]	12.993(5)	7.088(3)	7.449(3)	93.13(4)	684.9(3)
1.96[a]	12.975(3)	7.086(2)	7.447(2)	92.80(2)	683.9(2)
2.74[a]	12.927(3)	7.064(2)	7.437(2)	92.56(3)	678.4(2)
3.24[b]	12.889(5)	7.050(3)	7.427(3)	92.71(4)	674.1(4)
3.77[a]	12.862(3)	7.040(2)	7.421(3)	92.37(3)	671.3(2)
4.48[b]	12.809(4)	7.020(2)	7.413(3)	92.41(4)	666.0(3)
5.55[a]	12.745(3)	6.997(2)	7.396(3)	91.95(4)	659.1(3)
6.27[b]	12.711(4)	6.979(2)	7.387(3)	92.07(4)	654.9(3)
7.92[b]	12.620(5)	6.951(3)	7.356(4)	91.83(5)	645.0(4)
8.09[a]	12.616(4)	6.948(2)	7.360(5)	91.63(5)	644.9(4)
9.58[b]	12.547(4)	6.910(1)	7.342(2)	91.62(2)	636.3(1)
10.50[a]	12.538(5)	6.921(3)	7.332(6)	91.44(6)	636.0(5)
11.32[b]	12.483(4)	6.897(2)	7.323(4)	91.38(4)	630.2(3)
12.59[a]	12.486(7)	6.899(4)	7.321(9)	91.22(10)	630.5(8)
13.39[b]	12.433(4)	6.879(2)	7.310(5)	91.13(5)	625.1(4)
14.48[a]	12.424(8)	6.884(4)	7.306(10)	91.01(11)	624.7(9)
14.83[b]	12.394(5)	6.866(3)	7.297(6)	91.05(7)	620.9(5)
15.64[b]	12.327(4)	6.861(3)	7.307(1)	90.92(1)	617.9(3)
17.04[a]	12.347(10)	6.857(5)	7.278(13)	90.90(14)	616.1(11)

Notes: [a]Measured at 4W2, BSRF in China.
[b]Measured at BL-18C, KEK in Japan.

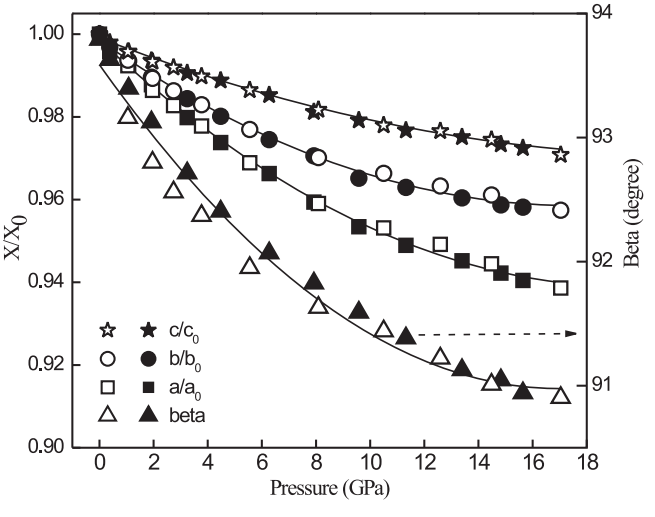

Figure 3. Unit-cell parameters of $BaWO_4$-II phase as a function of pressure. Data normalized with respect to room-pressure values except the beta parameter. The solid and empty symbols represent the data measured at BL-18C, KEK in Japan and 4W2, BSRF in China, respectively.

to the cell volume (662.247 Å^3) at 6 GPa and 700 K, and the correlative empty triangle represents the cell volume (657.457 Å^3) at 6 GPa and 298 K, which was obtained according to the linear coefficient of thermal volume expansion (1.8×10^{-5} K^{-1}) of $BaWO_4$-II at 6 GPa given by Lacomba-Perales *et al*. [9]. We find that the earlier reported pressure–volume data [9] agree better with our experimental results when the effect of temperature was eliminated.

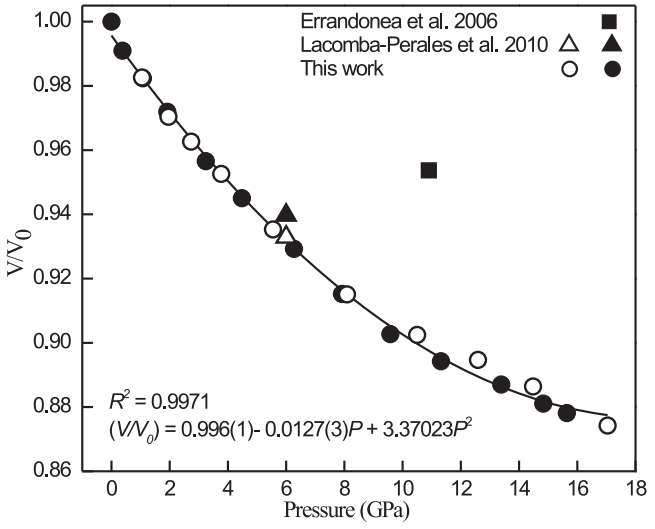

Figure 4. Pressure dependence of relative volume (V/V_0) for $BaWO_4$-II phase. The solid line is the polynomial fitting to the two sets of P–V data (solid circles at BL-18C and empty circles at 4W2). The square and triangle represent the earlier reported X-ray diffraction data [6,9].

The solid square in Figure 4 represents the cell volume (672.100 $Å^3$) for the previously reported high pressure phase of $BaWO_4$ at 10.9 GPa and room temperature [6]. Because the quality of the ADXRD patterns collected from the post-fergusonite structure of $BaWO_4$ did not allow a Rietveld refinement, the author analyzed it using the Le Bail extraction technique considering some candidate structures and chose the most likely $BaWO_4$-II structure. However, this point deviates far from the solid curve of polynomial fitting of $BaWO_4$-II. Therefore, the post-fergusonite structure of $BaWO_4$ at the RT-HP experiments may not adopt the $BaWO_4$-II structure. This assumption will provide new approach for solving the contradiction of reversibility and irreversibility of the $BaWO_4$-II [5,6].

4. Conclusions

The pure $BaWO_4$-II has been synthesized at 5 GPa and 610°C. *In situ* synchrotron X-ray diffraction of $BaWO_4$-II has been investigated at room temperature up to 17 GPa in a DAC. The ADXRD spectra measured by the authors are very different to those of Ref. [6, Figures 1 and 4] and they are very similar to the $BaWO_4$-II spectra reported in Ref. [9, Figure 8]. No phase transition was observed in the pressure range studied. The elastic moduli of the $BaWO_4$-II phase, obtained from fitting data to a third-order Birch–Murnaghan equation of state (K' fixed at 4) are: $K_0 = 86.2 \pm 1.9$ GPa, $K_0(a) = 56.0 \pm 0.9$ GPa, $K_0(b) = 85.3 \pm 2.4$ GPa, and $K_0(c) = 146.1 \pm 3.2$ GPa. These data confirm the elasticity of $BaWO_4$-II: the a-axis is 2.61 times more compressible than the c-axis and 1.71 times more compressible than the b-axis. The beta angle steadily decreases to the value of 90.90° with increasing pressures.

Acknowledgment

The authors are grateful for the support from the Knowledge Innovation Project of Chinese Academy of Sciences (KJCX2-SW-N20) and the National Natural Science Foundation of China (90714011). We also thank the help from High Pressure Research Group, BSRF, China and BL-18C, KEK, Japan. This is contribution No. IS-1439 from GIGCAS.

References

[1] A. Sleight, *Accurate cell dimensions for ABO_4 molybdates and tungstates*, Acta Crystallogr B 28 (1972), pp. 2899–2902.

[2] O. Fukunaga and S. Yamaoka, *Phase-transformations in ABO_4 type compounds under high-pressure*, Phys. Chem. Miner. 5 (1979), pp. 167–177.

[3] D. Errandonea and F.J. Manjon, *Pressure effects on the structural and electronic properties of ABX_4 scintillating crystals*, Prog. Mater. Sci. 53 (2008), pp. 711–773.

[4] I. Kawada, K. Kato, and T. Fujita, *$BaWO_4$-II – high-pressure form*, Acta Crystallogr B 30 (1974), pp. 2069–2071.

[5] T. Fujita, S. Yamaoka, and O. Fukunaga, *Pressure-induced phase-transformation in $BaWO_4$*, Mater. Res. Bull. 9 (1974), pp. 141–146.

[6] D. Errandonea, J. Pellicer-Porres, F.J. Manjon, A. Segura, C. Ferrer-Roca, R.S. Kumar, O. Tschauner, J. Lopez-Solano, P. Rodriguez-Hernandez, S. Radescu, A. Mujica, A. Munoz, and G. Aquilanti, *Determination of the high-pressure crystal structure of $BaWO_4$ and $PbWO_4$*, Phys. Rev. B 73 (2006), pp. 224103-1–15.

[7] F.J. Manjon, D. Errandonea, N. Garro, J. Pellicer-Porres, P. Rodriguez-Hernandez, S. Radescu, J. Lopez-Solano, A. Mujica, and A. Munoz, *Lattice dynamics study of scheelite tungstates under high pressure I. $BaWO_4$*, Phys. Rev. B 74 (2006), pp. 144111-1–17.

[8] D.Y. Tan, W.S. Xiao, W.G. Zhou, M.S. Song, X.L. Xiong, and M. Chen, *Raman investigation of $BaWO_4$-II phase under hydrostatic pressures up to 14.8 GPa*, Chin. Phys. Lett. 26 (2009), pp. 046301-1–4.

[9] R. Lacomba-Perales, D. Martinez-Garcia, D. Errandonea, Y. Le Godec, J. Philippe, G. Le Marchand, J.C. Chervin, A. Polian, A. Munoz, and J. Lopez-Solano, *Experimental and theoretical investigation of the stability of the monoclinic $BaWO_4$-II phase at high pressure and high temperature*, Phys. Rev. B 81 (2010), pp. 144117-1–10.

[10] H.K. Mao, J. Xu, and P.M. Bell, *Calibration of the ruby pressure gauge to 800-kbar under quasi-hydrostatic conditions*, J. Geophys. Res. 91 (1986), pp. 4673–4676.

[11] B.H. Toby, *EXPGUI, a graphical user interface for GSAS*, J. Appl. Crystallogr. 34 (2001), pp. 210–213.

[12] R.J. Angel, *Equations of state*, High-temp. High-pressure Cryst. Chem. 41 (2000), pp. 35–59.

[13] F. Birch, *Finite elastic strain of cubic crystals*, Phys. Rev. 71 (1947), pp. 809–824.

[14] S. Klotz, J.C. Chervin, P. Munsch, and G. Le Marchand, *Hydrostatic limits of 11 pressure transmitting media*, J. Phys. D Appl. Phys. 42 (2009), pp. 075413-1–7.

[15] V. Panchal, N. Garg, A.K. Chauhan, B. Sangeeta, and S.M. Sharma, *High pressure phase transitions in $BaWO_4$*, Solid State Commun. 130 (2004), pp. 203–208.